






Article

Secoiridoid Glucosides and Anti-Inflammatory Constituents from the Stem Bark of *Fraxinus chinensis*

Hao-Chiun Chang^{1,2,†}, Shih-Wei Wang^{3,4,†}, Chin-Yen Chen⁵, Tsong-Long Hwang^{6,7,8},
Ming-Jen Cheng⁹, Ping-Jyun Sung^{4,10}, Kuang-Wen Liao^{2,11} and Jih-Jung Chen^{12,13,*}

¹ Department of Orthopaedics, MacKay Memorial Hospital, Taipei 10449, Taiwan; Changhaochiun@gmail.com

² Ph.D. Degree Program of Biomedical Science and Engineering, National Chiao Tung University, Hsinchu City 30068, Taiwan; liaonms@g2.nctu.edu.tw

³ Department of Medicine, MacKay Medical College, New Taipei City 25242, Taiwan; shihwei@mmc.edu.tw

⁴ Graduate Institute of Natural Products, Kaohsiung Medical University, Kaohsiung 80708, Taiwan; pjsung@nmmmba.gov.tw

⁵ Graduate Institute of Pharmaceutical Technology, Tajen University, Pingtung 90741, Taiwan; jjc8506674@gmail.com

⁶ Graduate Institute of Natural Products, School of Traditional Chinese Medicine, College of Medicine, Chang Gung University, Taoyuan 33303, Taiwan; htl@mail.cgu.edu.tw

⁷ Research Center for Food and Cosmetic Safety, Graduate Institute of Health Industry Technology, College of Human Ecology, Chang Gung University of Science and Technology, Taoyuan 33303, Taiwan

⁸ Department of Anesthesiology, Chang Gung Memorial Hospital, Taoyuan 333, Taiwan

⁹ Bioresource Collection and Research Center (BCRC), Food Industry Research and Development Institute (FIRDI), Hsinchu 30062, Taiwan; cmj@firdi.org.tw

¹⁰ National Museum of Marine Biology and Aquarium, Pingtung 94450, Taiwan

¹¹ Institute of Molecular Medicine and Bioengineering, National Chiao Tung University, Hsinchu City 30068, Taiwan

¹² Faculty of Pharmacy, School of Pharmaceutical Sciences, National Yang-Ming University, Taipei 11221, Taiwan

¹³ Department of Medical Research, China Medical University Hospital, China Medical University, Taichung 40402, Taiwan

* Correspondence: chenjj@ym.edu.tw; Tel.: +886-2-2826-7195

† These authors contributed equally to this manuscript.

Academic Editor: Phurpa Wangchuk

Received: 14 November 2020; Accepted: 9 December 2020; Published: 14 December 2020



Abstract: Qin Pi (*Fraxinus chinensis* Roxb.) is commercially used in healthcare products for the improvement of intestinal function and gouty arthritis in many countries. Three new secoiridoid glucosides, (8E)-4''-O-methyliligstroside (1), (8E)-4''-O-methyl-demethyliligstroside (2), and 3'',4''-di-O-methyl-demethyloleuropein (3), have been isolated from the stem bark of *Fraxinus chinensis*, together with 23 known compounds (4–26). The structures of the new compounds were established by spectroscopic analyses (1D, 2D NMR, IR, UV, and HRESIMS). Among the isolated compounds, (8E)-4''-O-methyliligstroside (1), (8E)-4''-O-methyl-demethyliligstroside (2), 3'',4''-di-O-methyl-demethyloleuropein (3), oleuropein (6), aesculetin (9), isoscapoletin (11), aesculetin dimethyl ester (12), fraxetin (14), tyrosol (21), 4-hydroxyphenethyl acetate (22), and (+)-pinoreosin (24) exhibited inhibition ($IC_{50} \leq 7.65 \mu\text{g/mL}$) of superoxide anion generation by human neutrophils in response to formyl-L-methionyl-L-leucyl-L-phenylalanine/cytochalasin B (fMLP/CB). Compounds 1, 9, 11, 14, 21, and 22 inhibited fMLP/CB-induced elastase release with $IC_{50} \leq 3.23 \mu\text{g/mL}$. In addition, compounds 2, 9, 11, 14, and 21 showed potent inhibition with IC_{50} values $\leq 27.11 \mu\text{M}$, against lipopolysaccharide (LPS)-induced nitric oxide (NO) generation. The well-known proinflammatory cytokines, tumor necrosis factor-alpha (TNF- α) and interleukin 6 (IL-6), were also inhibited by compounds 1, 9, and 14. Compounds 1, 9, and 14 displayed an anti-inflammatory effect against NO, TNF- α , and IL-6 through the inhibition of activation of MAPKs and $I\kappa B\alpha$ in LPS-activated

macrophages. In addition, compounds **1**, **9**, and **14** stimulated anti-inflammatory M2 phenotype by elevating the expression of arginase 1 and Krüppel-like factor 4 (KLF4). The above results suggested that compounds **1**, **9**, and **14** could be considered as potential compounds for further development of NO production-targeted anti-inflammatory agents.

Keywords: *Fraxinus chinensis*; Oleaceae; stem bark; secoiridoid; anti-inflammatory activity

1. Introduction

Fraxinus chinensis Roxb. (Oleaceae) is a deciduous tree distributed in China, Japan, Korea, Russia, and Vietnam [1]. Its stem bark, called “Qin Pi”, is used as a health food or herbal supplement for improving intestinal function in Asia and America. The Oleaceae family is a rich source of secoiridoid glucosides [2]. A number of secoiridoid glucosides [2–6], coumarins [5,6], phenylpropenoids [5,6], lignans [6], and benzofuran derivatives [6] have been reported from the genus *Fraxinus*. These derivatives have been reported to exhibit several biological activities, such as antidiabetic [4], anti-inflammatory [4], immunosuppressive [4], anticancer [4], and quinone reductase-inducing activities [6]. *F. chinensis* has been found to be an active material by screening for anti-inflammatory effect of many natural sources. Three new secoiridoid glucosides, (8*E*)-4''-*O*-methyliligstroside (**1**), (8*E*)-4''-*O*-methyldemethyliligstroside (**2**), and 3'',4''-di-*O*-methyldemethyloleuropein (**3**), and 23 known compounds (**4–26**) have been isolated and confirmed from the stem bark of *F. chinensis*. This report depicts the structural elucidation of three new compounds **1–3** and the inhibitory activities of all isolated compounds against fMLP/CB-induced O₂^{•−} and elastase release and against LPS-induced NO generation.

2. Results and Discussion

2.1. Isolation and Structural Elucidation

Separation of the EtOAc-soluble fraction of an MeOH extract of stem bark of *F. chinensis* by silica gel chromatography and preparative thin-layer chromatography (TLC) afforded three new (**1–3**) and 23 known compounds (**4–26**) (Figure 1).

Compound **1** was obtained as yellowish oil and the molecular formula was determined to be C₂₆H₃₄O₁₂ by ESI-MS [*m/z* 561 [M + Na]⁺] (Figure S1) and HR-ESI-MS [*m/z* 561.1950 [M + Na]⁺ (calcd for C₂₆H₃₄NaO₁₂, 561.1948)] (Figure S2). The IR spectrum showed the presence of hydroxyl (3402 cm^{−1}) and carbonyl (1727 and 1709 cm^{−1}) groups. Analysis of the ¹H (Table 1 and Figure S3) and ¹³C NMR (Table 2 and Figure S4) data of **1** revealed signals for a 4-methoxyphenethoxy group [δ_{H} 2.85 (2H, t, *J* = 7.0 Hz, H- β), 3.76 (3H, s, OMe-4''), 4.12, 4.24 (each 1H, each dt, *J* = 10.5, 7.0 Hz, H- α), 6.85 (2H, d, *J* = 9.0 Hz, H-3'' and H-5''), 7.15 (2H, d, *J* = 9.0 Hz, H-2'' and H-6''); δ_{C} 35.2 (C- β), 55.9 (OMe-4''), 67.0 (C- α), 115.1 (C-3'' and C-5''), 131.2 (C-2'' and C-6''), 131.5 (C-1''), 160.0 (C-4'')], a secoiridoid moiety [δ_{H} 1.62 (3H, dd, *J* = 7.0, 1.0 Hz, H-10), 2.44 (1H, dd, *J* = 14.0, 9.5 Hz, H-6), 2.69 (1H, dd, *J* = 14.0, 5.0 Hz, H-6), 3.71 (3H, s, OMe-11), 3.95 (1H, dd, *J* = 9.5, 5.0 Hz, H-5), 5.92 (1H, br s, H-1), 6.06 (1H, br q, *J* = 7.0 Hz, H-8), 7.51 (1H, s, H-3); δ_{C} 13.7 (C-10), 32.0 (C-5), 41.3 (C-6), 52.1 (C-CH₃OCO-4), 95.3 (C-1), 109.5 (C-4), 125.1 (C-8), 130.5 (C-9), 155.3 (C-3), 168.9 (CH₃OCO-4), 173.4 (C-7)], and a β -glucose moiety [δ_{H} 3.28–3.36 (3H, m, H-2', H-4', and H-5'), 3.42 (1H, dd, *J* = 8.5, 8.5 Hz, H-3'), 3.66 (1H, dd, *J* = 12.0, 5.5 Hz, H-6'), 3.88 (1H, dd, *J* = 12.0, 1.5 Hz, H-6'), 4.80 (1H, d, *J* = 7.5 Hz, H-1'); δ_{C} 62.9 (C-6'), 71.7 (C-4'), 74.9 (C-2'), 78.1 (C-3'), 78.6 (C-5'), 101.0 (C-1')]. These data were nearly identical with those of (8*E*)-ligstroside (**5**) [7], except that a methoxy group [δ_{H} 3.76 (3H, s); δ_{C} 55.9] at C-4'' of **1** replaced the 4''-hydroxy group of (8*E*)-ligstroside (**5**) [7]. This was supported by NOESY correlations between OMe-4'' (δ_{H} 3.76) and H-3''/H-5'' (δ_{H} 6.85) and by HMBC correlation between OMe-4'' (δ_{H} 3.76) and C-4'' (δ_{C} 160.0) (Figure 2). The *E*-configuration at C-8 was confirmed by NOESY

correlation between H-5 and H-10. In the NOESY spectrum, H-1 (δ 5.92) had the correlation with H-6 (δ 2.44) and had no correlation with H-5 (δ 3.95), which indicated the relative configurations of H-1 and H-5 as α and β , respectively. The position of each substituent was supported by NOESY correlations (Figure 2) between H-1 (δ_{H} 5.92)/H-6 (δ_{H} 2.44), H-1 (δ_{H} 5.92)/H-8 (δ_{H} 6.06), H-5 (δ_{H} 3.95)/H-10 (δ_{H} 1.62), H-1' (δ_{H} 4.80)/H-3' (δ_{H} 3.42), H- β (δ_{H} 2.85)/H-2'' (δ_{H} 7.15), and H-3'' (δ_{H} 6.85)/OMe-4'' (δ_{H} 3.76) and by HMBC correlation (Figure 2) between H-1 (δ_{H} 5.92)/C-8 (δ_{C} 125.1), H-1 (δ_{H} 5.92)/C-1' (δ_{C} 101.0), H-3 (δ_{H} 7.51)/C-1 (δ_{C} 95.3), H-3 (δ_{H} 7.51)/C-5 (δ_{C} 32.0), H-5 (δ_{H} 3.95)/C-7 (δ_{C} 173.4), H-5 (δ_{H} 3.95)/C-11 (δ_{C} 168.9), H-10 (δ_{H} 1.62)/C-9 (δ_{C} 130.5), OMe-11 (δ_{H} 3.71)/C-11 (δ_{C} 168.9), H- α (δ_{H} 4.12)/C-7 (δ_{C} 173.4), H- α (δ_{H} 4.12)/C-1'' (δ_{C} 131.5), H- β (δ_{H} 2.85)/C-2'',6'' (δ_{C} 131.2), H-3'',5'' (δ_{H} 6.85)/C-1'' (δ_{C} 131.5), and OMe-4'' (δ_{H} 3.76)/C-4'' (δ_{C} 160.0). The full assignment of ^1H and ^{13}C NMR resonances was supported by DEPT (Figure S5), ^1H - ^1H COSY (Figure S6), NOESY (Figure S7), HMBC (Figure S8), and HSQC (Figure S9) spectral analyses. According to the above data, the structure of **1** was elucidated as (8*E*)-4''-*O*-methyligstroside.

Table 1. ^1H -NMR data for compounds **1–3** (δ in ppm, *J* in Hz).

Position	1 ^a	2 ^a	3 ^a
1	5.92 br s	5.87 br s	5.86 br s
3	7.51 s	7.39 s	7.38 s
5	3.95 dd (9.5, 5.0)	4.01 dd (9.5, 5.0)	4.00 dd (9.5, 4.5)
6	2.44 dd (14.0, 9.5) 2.69 dd (14.0, 5.0)	2.41 dd (14.0, 9.5) 2.79 dd (14.0, 4.5)	2.41 dd (14.0, 9.5) 2.80 dd (14.0, 4.5)
8	6.06 br q (7.0)	6.05 br q (7.0)	6.06 br q (7.0)
10	1.62 dd (7.0, 1.0)	1.66 dd (7.0, 1.0)	1.66 dd (7.0, 1.0)
α	4.12 dt (10.5, 7.0) 4.24 dt (10.5, 7.0)	4.11 dt (10.5, 7.0) 4.23 dt (10.5, 7.0)	4.15 dt (10.5, 7.0) 4.27 dt (10.5, 7.0)
β	2.85 t (7.0)	2.85 t (7.0)	2.86 t (7.0)
1'	4.80 d (7.5)	4.80 d (8.0)	4.80 d (8.0)
2'	3.28–3.36 m	3.29–3.35 m	3.28–3.36 m
3'	3.42 dd (8.5, 8.5)	3.41 dd (9.0, 8.5)	3.41 dd (8.5, 8.5)
4'	3.28–3.36 m	3.29–3.35 m	3.28–3.36 m
5'	3.28–3.36 m	3.29–3.35 m	3.28–3.36 m
6'	3.66 dd (12.0, 5.5) 3.88 dd (12.0, 1.5)	3.67 dd (12.0, 5.5) 3.88 dd (12.0, 1.5)	3.66 dd (12.0, 5.5) 3.88 dd (12.0, 1.5)
2''	7.15 d (9.0)	7.15 d (9.0)	6.86 d (2.0)
3''	6.85 d (9.0)	6.85 d (9.0)	
5''	6.85 d (9.0)	6.85 d (9.0)	6.88 d (8.5)
6''	7.15 d (9.0)	7.15 d (9.0)	6.79 dd (8.5, 2.0)
OMe-11	3.71 s		
OMe-3''			3.82 s
OMe-4''	3.76 s	3.76 s	3.80 s

^a Measured in CD₃OD at 500 MHz.

Compound **2** was obtained as amorphous powder. The ESI-MS (Figure S10) afforded a sodium adduct ion $[\text{M} + \text{Na}]^+$ at *m/z* 547, implying a molecular formula of C₂₅H₃₂O₁₂, which was confirmed by the HR-ESI-MS mass spectrum (*m/z* 547.1787 $[\text{M} + \text{Na}]^+$, calcd for C₂₅H₃₂O₁₂Na, 547.1791) (Figure S11). The presence of hydroxyl (3334 cm⁻¹) and carbonyl (1728 and 1707 cm⁻¹) groups were evident from the IR spectrum. The ^1H (Table 1 and Figure S12) and ^{13}C NMR (Table 2 and Figure S13) data of **2** were very similar to those of demethyligstroside [3], except that a methoxy group [δ_{H} 3.76 (3H, s)] at C-4'' in **2** replaced the 4''-hydroxy group of demethyligstroside [3]. This was supported by NOESY correlations between OMe-4'' (δ_{H} 3.76) and H-3''/H-5'' (δ_{H} 6.85) and by HMBC correlation between OMe-4'' (δ_{H} 3.76) and C-4'' (δ_{C} 160.0) (Figure 3). The relative configuration of **2** was assigned by NOESY spectrum, which showed correlation between H-1 (δ 5.87) and H-6 (δ 2.41), suggesting that H-5 was on the β configuration, and H-1 was on the α configuration. The *E*-configuration at C-8 was confirmed by NOESY correlation between H-5 and H-10. The full assignment of ^1H and ^{13}C NMR resonances

was supported by DEPT (Figure S14), ^1H - ^1H COSY (Figure S15), NOESY (Figure 3 and Figure S16), HMBC (Figure 3 and Figure S17), and HSQC (Figure S18) spectral analyses. Thus, the structure of **2** was established as shown in Figure 1, and named (8*E*)-4''-*O*-methylidemethyligstroside.

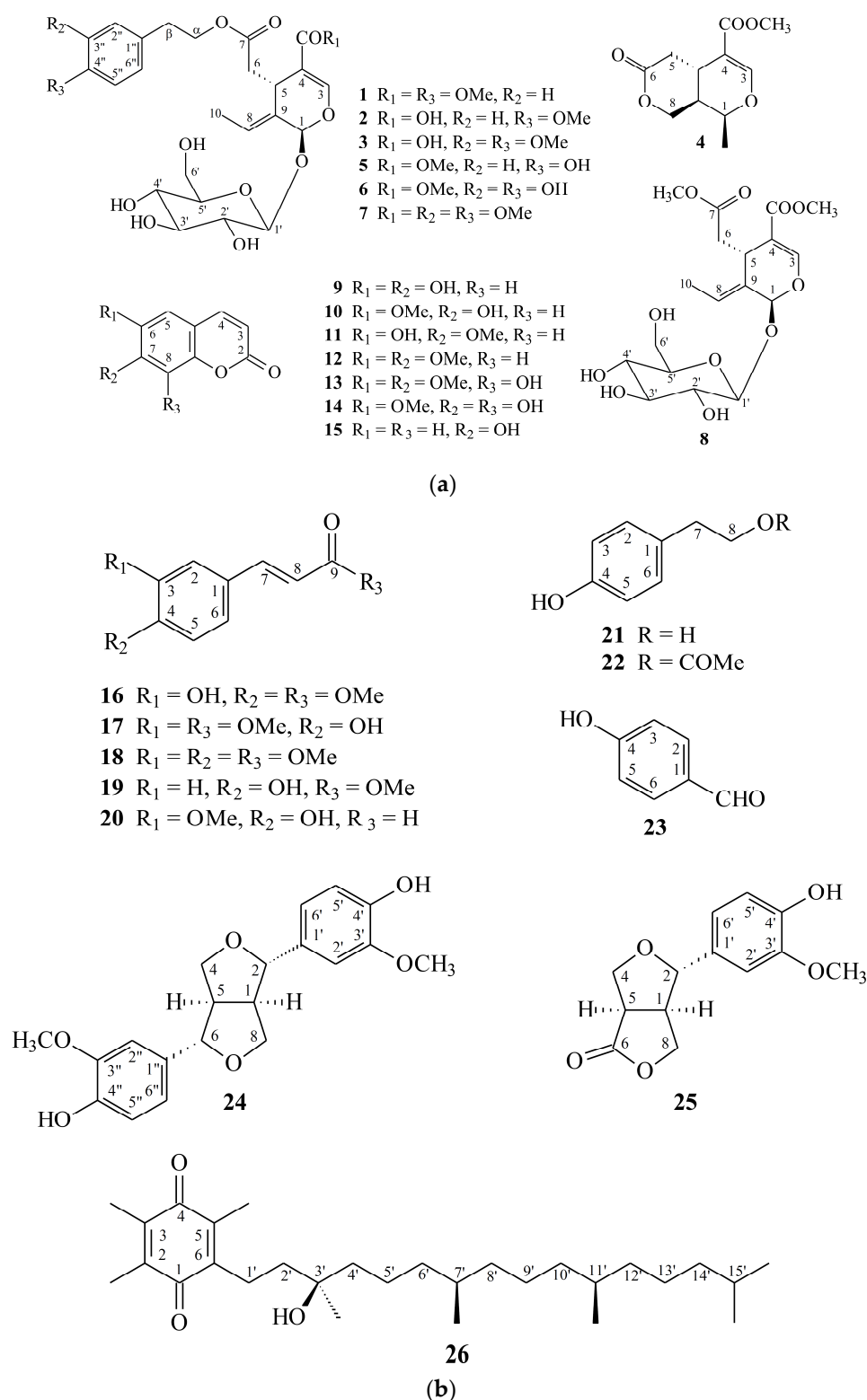
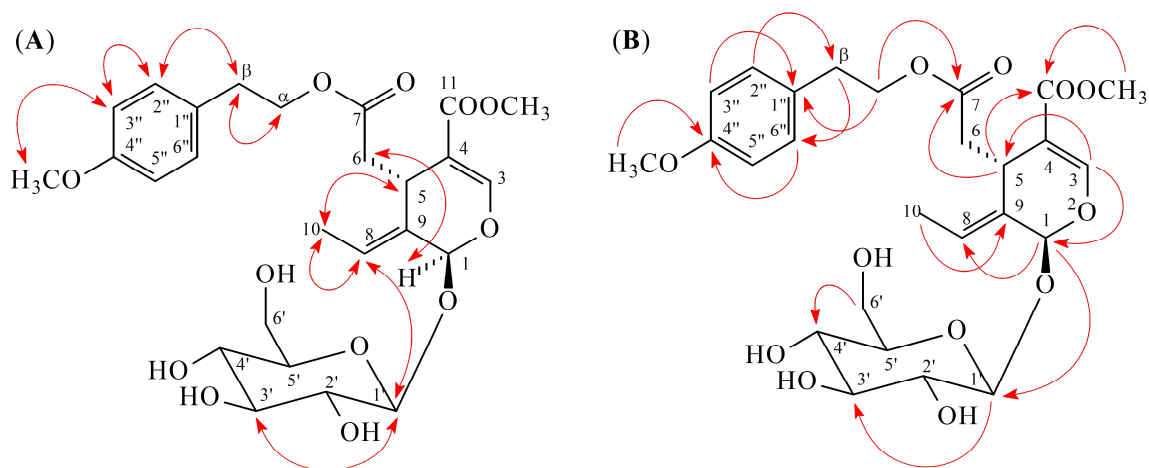


Figure 1. The chemical structures of compounds **1**–**15** (a) and **16**–**26** (b) isolated from *F. chinensis*.

Table 2. ^{13}C -NMR data for compounds 1–3 (δ in ppm).

Position	1 ^a	2 ^a	3 ^a
1	95.3	95.0	95.3
3	155.3	152.8	155.3
4	109.5	110.2	109.5
5	32.0	31.9	32.0
6	41.3	41.3	41.4
7	173.4	173.3	173.4
8	125.1	124.6	125.0
9	130.5	130.7	130.6
10	13.7	13.6	13.7
11	168.9	171.0	168.8
α	67.0	66.9	66.9
β	35.2	35.2	35.7
1'	101.0	101.0	101.0
2'	74.9	74.9	74.9
3'	78.1	78.1	78.1
4'	71.7	71.6	71.6
5'	78.6	78.6	78.6
6'	62.9	62.9	62.9
1''	131.5	131.5	132.4
2''	131.2	131.2	114.1
3''	115.1	115.1	150.5
4''	160.0	160.0	149.3
5''	115.1	115.1	113.4
6''	131.2	131.2	122.6
OMe-11	52.1		
OMe-3''			56.7
OMe-4''	55.9	55.9	56.7

^a Measured in CD_3OD at 125 MHz.**Figure 2.** Key NOESY (A) and HMBC (B) correlations of 1.

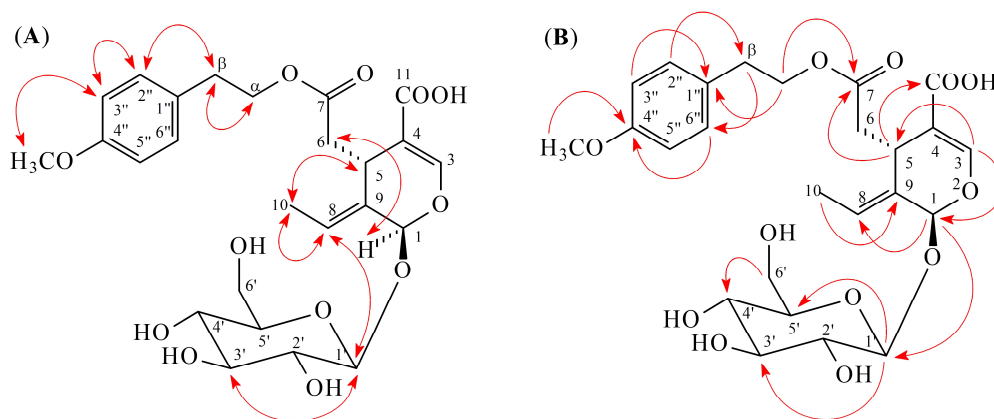


Figure 3. Key NOESY (A) and HMBC (B) correlations of **2**.

Compound **3** was isolated as amorphous powder. Its molecular formula, $C_{26}H_{34}O_{13}$, was determined on the basis of the positive ESI-MS at m/z 577 $[M + Na]^+$ (Figure S19) and HR-ESI-MS at m/z 577.1892 $[M + Na]^+$ (calcd 577.1897) (Figure S20) and was supported by the 1H , ^{13}C , and DEPT NMR data. The IR absorption bands of **3** revealed the presence of hydroxyl (3350 cm^{-1}) and carbonyl (1721 and 1698 cm^{-1}) functions. The 1H (Table 1 and Figure S21) and ^{13}C NMR (Table 2 and Figure S22) data of **3** were similar to those of **2**, except that a 3,4-dimethoxyphenyl group [δ_H 3.80 (3H, s, OMe-4''), 3.82 (3H, s, OMe-3''), 6.79 (1H, dd, $J = 8.5, 2.0$ Hz, H-6''), 6.86 (1H, d, $J = 2.0$ Hz, H-2''), 6.88 (1H, d, $J = 8.5$ Hz, H-5''); δ_C 56.7 (OMe-3''), 56.7 (OMe-4''), 113.3 (C-5''), 114.1 (C-2''), 122.6 (C-6''), 132.5 (C-1''), 149.3 (C-4''), 150.5 (C-3'')] at C- β in **3** replaced the 4-methoxyphenyl group at C- β of **2**. This was supported by NOESY correlations between OMe-3'' (δ_H 3.82) and H-2'' (δ_H 6.86) and by HMBC correlation between OMe-3'' (δ_H 3.82) and C-3'' (δ_C 150.5) (Figure 4). The relative configuration of **3** was assumed to be the same as that of **2** based on the NOESY correlation between H-1 (δ_H 5.86) and H-6 (δ_H 2.41). The *E*-configuration at C-8 was confirmed by NOESY correlation between H-5 and H-10. The full assignment of 1H and ^{13}C NMR resonances was further confirmed by DEPT (Figure S23), 1H - 1H COSY (Figure S24), NOESY (Figure 4 and Figure S25), HMBC (Figure 4 and Figure S26), and HSQC (Figure S27) data. Consequently, the structure of compound **3** was established as 3'',4''-di-*O*-methyldemethylleuropein.

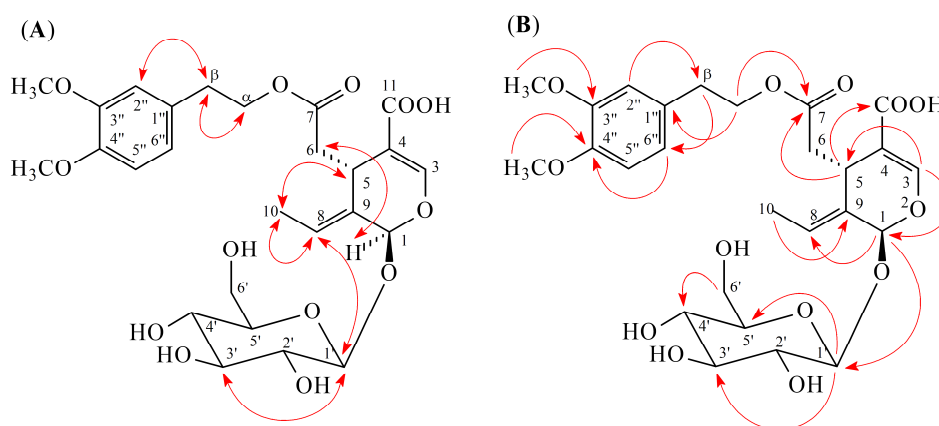


Figure 4. Key NOESY (A) and HMBC (B) correlations of **3**.

2.2. Structure Identification of the Known Isolates

The known isolates were readily identified by a comparison of their physical and spectroscopic data (UV, IR, 1H NMR, $[\alpha]_D$, and MS) with those of authentic samples or literature values. They include a pyran derivative, fraxilatone (**4**) [8], four secoiridoids, (*8E*)-ligstroside (**5**) [7,9], oleuropein (**6**) [9],

(8*E*)-3'',4''-di-*O*-methyloleuropein (7) [10], and oleoside methyl ester (8) [11], seven coumarins, aesculetin (9) [12], scopoletin (10) [12,13], isoscopoletin (11) [12,14], aesculetin dimethyl ester (12) [12,15], fraxidin (13) [16,17], fraxetin (14) [18], and umbelliferone (15) [19], five phenylpropanoids, methyl isoferulate (16) [20], methyl ferulate (17) [21], methyl 3,4-dimethoxycinnamate (18) [22], methyl (*E*)-*p*-coumarate (19) [23], and (*E*)-ferulaldehyde (20) [24], two phenylethanoids, tyrosol (21) [25] and 4-hydroxyphenethyl acetate (22) [26], a benzenoid, *p*-hydroxybenzaldehyde (23) [27], two lignans, (+)-pinoresinol (24) [28] and (+)-salicifoliol (25) [29], and a α -tocopheranoid: α -tocopheryl quinone (26) [30].

2.3. Biological Studies

Reactive oxygen species (ROS) (e.g., hydrogen peroxide and superoxide anion ($O_2^{\bullet-}$)) and granule proteases (e.g., elastase, proteinase-3, and cathepsin G) produced by human neutrophils are involved in the pathogenesis of a variety of inflammatory diseases [31–33]. The effects on neutrophil proinflammatory responses of isolated compounds from the stem bark of *F. chinensis* were evaluated by suppressing fMLP/CB-induced superoxide radical anion ($O_2^{\bullet-}$) generation and elastase release by human neutrophils. The inhibitory activity data on human neutrophil proinflammatory responses are shown in Table 3. Diphenylethylidone and phenylmethylsulfonyl fluoride were used as positive controls for $O_2^{\bullet-}$ generation and elastase release, respectively. From the results of our biological tests, the following conclusions can be drawn: (a) (8*E*)-4''-*O*-methylglistroside (1), (8*E*)-4''-*O*-methyldemethylglistroside (2), 3'',4''-di-*O*-methyldemethyloleuropein (3), oleuropein (6), aesculetin (9), isoscopoletin (11), aesculetin dimethyl ester (12), fraxetin (14), tyrosol (21), 4-hydroxyphenethyl acetate (22), and (+)-pinoresinol (24) showed potent inhibition ($IC_{50} \leq 7.65 \mu\text{g/mL}$) of $O_2^{\bullet-}$ generation by neutrophils in response to fMLP/CB; (b) (8*E*)-4''-*O*-methylglistroside (1), aesculetin (9), isoscopoletin (11), fraxetin (14), tyrosol (21), and 4-hydroxyphenethyl acetate (22) displayed potent inhibition ($IC_{50} \leq 3.23 \mu\text{g/mL}$) against fMLP-induced elastase release; (c) secoiridoid glucoside, (8*E*)-4''-*O*-methylglistroside (1) (with 4''-methoxy group) displayed more effective inhibition than its analogue, (8*E*)-glistroside (5) (with 4''-hydroxy group) against fMLP-induced $O_2^{\bullet-}$ generation and elastase release; (d) among the 6,7-disubstituted coumarin derivatives, aesculetin (9) (with 6,7-dihydroxy groups) exhibited more effective inhibition than its analogues, scopoletin (10) (with 7-hydroxy-6-methoxy groups), isoscopoletin (11) (with 6-hydroxy-7-methoxy groups), and aesculetin dimethyl ester (12) (with 6,7-dimethoxy groups) against fMLP-induced $O_2^{\bullet-}$ generation; (e) among the 6,7,8-trisubstituted coumarin derivatives, fraxetin (14) (with 7,8-dihydroxy-6-methoxy groups) displayed more effective inhibition than its analogue, fraxidin (13) (with 8-hydroxy-6,7-dimethoxy groups) against fMLP-induced $O_2^{\bullet-}$ generation and elastase release; (f) (8*E*)-4''-*O*-methylglistroside (1) and fraxetin (14) were the most effective among the isolated compounds, with IC_{50} values of 0.08 ± 0.01 and $0.50 \pm 0.10 \mu\text{g/mL}$, respectively, against fMLP-induced $O_2^{\bullet-}$ generation and elastase release.

Nitric oxide (NO) is a mediator in the inflammatory response involved in host defense. The anti-inflammatory effects of the compounds isolated from the stem bark of *F. chinensis* were also evaluated by suppressing lipopolysaccharide (LPS)-induced NO generation in macrophage cell line RAW264.7. The inhibitory activity data of the isolates 1–26 on NO generation by macrophages are shown in Table 4. Quercetin was used as the positive control. From the results of our anti-inflammatory assays, the following conclusions can be drawn: (a) (8*E*)-4''-*O*-methyldemethylglistroside (2), aesculetin (9), isoscopoletin (11), fraxetin (14), and tyrosol (21) showed potent inhibition with IC_{50} values $\leq 27.11 \mu\text{M}$, against lipopolysaccharide (LPS)-induced nitric oxide (NO) generation; (b) secoiridoid glucoside, (8*E*)-4''-*O*-methylglistroside (1) (with 4''-methoxy group) displayed more effective inhibition than its analogue, (8*E*)-glistroside (5) (with 4''-hydroxy group) against LPS-induced NO generation; (c) among the 6,7-disubstituted coumarin derivatives, aesculetin (9) (with 6,7-dihydroxy groups) and isoscopoletin (11) (with 6-hydroxy-7-methoxy groups) exhibited more effective inhibition than their analogues, scopoletin (10) (with 7-hydroxy-6-methoxy groups) and aesculetin dimethyl ester (12)

(with 6,7-dimethoxy groups) against LPS-induced NO generation; (d) among the 6,7,8-trisubstituted coumarin derivatives, fraxetin (**14**) (with 7,8-dihydroxy-6-methoxy groups) displayed more effective inhibition than its analogue, fraxidin (**13**) (with 8-hydroxy-6,7-dimethoxy groups) against LPS-induced NO generation; (e) (8E)-4''-O-Methylglistroside (**1**), aesculetin (**9**), and fraxetin (**14**) are the most effective among the isolated compounds, with IC₅₀ values of 12.38 ± 0.86, 9.36 ± 0.25, and 10.11 ± 0.47 μM, respectively, against LPS-induced NO production; (e) cytotoxic effects were tested using MTT experiment. The high cell viability (95, 98, and 97 %, respectively) of compounds **1**, **9**, and **14** at 50 μM showed that their inhibitory activities against LPS-induced NO generation did not arise from their cytotoxicities.

Table 3. Inhibitory effects of compounds 1–26 from the stem bark of *F. chinensis* on superoxide radical anion generation and elastase release by human neutrophils in response to fMet-Leu-Phe/cytochalasin B^a.

Compounds	Superoxide Anion	Elastase
	IC ₅₀ [μg/mL] ^b or (Inh %) ^c	
(8E)-4''-O-Methylglistroside (1)	0.08 ± 0.01 ***	2.57 ± 0.76 ***
(8E)-4''-O-Methyl demethylglistroside (2)	2.66 ± 0.33 ***	(42.92 ± 4.45) ***
3'',4''-Di-O-methyl demethyloleuropein (3)	5.22 ± 2.34 ***	(33.78 ± 1.64) ***
Olenoside A (4)	(8.67 ± 1.62) **	(19.87 ± 2.94) **
(8E)-Ligstroside (5)	(1.30 ± 1.88)	(26.58 ± 3.94) **
Oleuropein (6)	2.90 ± 0.46	(23.76 ± 0.50) ***
(8E)-3'',4''-Di-O-methyloleuropein (7)	(11.34 ± 6.05) *	(32.73 ± 4.35) **
Jaspolside methyl ester (8)	(14.39 ± 3.28) *	(20.54 ± 2.24) ***
Esculetin (9)	0.17 ± 0.03	2.41 ± 0.60
Copoletin (10)	(−0.91 ± 1.16)	(8.98 ± 1.68) **
Soscopoletin (11)	5.20 ± 1.52	3.23 ± 0.68
Esculetin dimethyl ester (12)	7.65 ± 1.62	(8.95 ± 2.94) *
Raxidin (13)	(8.95 ± 2.94) *	(12.14 ± 1.91) **
Raxetin (14)	0.19 ± 0.01	0.50 ± 0.10
Umbelliferone (15)	(3.38 ± 1.99)	(27.92 ± 4.88)
Methyl isoferulate (16)	(9.03 ± 1.65) **	(−2.76 ± 0.84) *
Methyl ferulate (17)	(23.02 ± 4.18) **	(24.12 ± 4.58) **
Methyl 3,4-dimethoxycinnamate (18)	(42.90 ± 3.97) ***	(7.05 ± 0.68) ***
Methyl (E)-p-coumarate (19)	(8.01 ± 0.66) ***	(20.30 ± 3.37) **
(E)-Ferulaldehyde (20)	(31.40 ± 7.95) **	(38.61 ± 3.64) ***
Tyrosol (21)	4.93 ± 0.19	2.64 ± 0.22
4-Hydroxyphenethyl acetate (22)	2.50 ± 0.35	3.03 ± 0.48
p-Hydroxybenzaldehyde (23)	(16.16 ± 2.03) **	(24.35 ± 4.45) **
(+)-Pinoresinol (24)	2.01 ± 0.38	(42.37 ± 2.06) ***
(+)-Salicifoliol (25)	(3.70 ± 2.59)	(9.14 ± 1.58) **
α-Tocopheryl quinone (26)	(17.88 ± 2.82) **	(11.35 ± 4.41)
Diphenyleneiodonium (DPI) ^d	0.52 ± 0.19 ***	-
Phenylmethylsulfonfyl fluoride (PMSF) ^d	-	34.4 ± 5.1 ***

^a Results are displayed as mean ± SEM (*n* = 3) of three independent experiments. ^b Concentration necessary for 50% inhibition (IC₅₀). If IC₅₀ value of tested compound was <10 μg/mL, it was presented as IC₅₀ [μg/mL]. ^c Percentage of inhibition (Inh %) at 10 μg/mL. If IC₅₀ value of tested compound was ≥10 μg/mL, it was displayed as Inh % at 10 μg/mL. ^d DPI and PMSF were employed as positive controls for superoxide anion (O₂^{•−}) production and elastase release, respectively. * *p* < 0.05 compared with the control. ** *p* < 0.01 compared with the control. *** *p* < 0.001 compared with the control.

The results of enzyme-linked immunosorbent assay (ELISA) showed that (8E)-4''-O-methylglistroside (**1**), aesculetin (**9**), and fraxetin (**14**) obviously suppressed TNF-α and IL-6 production in a concentration-dependent manner in RAW264.7 macrophages (Figure 5). Andrographolide was used as positive control. The action mechanisms of **1**, **9**, and **14** in macrophages were further investigated. Mitogen-activated protein kinases (MAPKs) and IκBα are the downstream signaling of LPS in macrophage cell line RAW264.7. Compounds **1**, **9**, and **14** (10 μM) caused a significant reduction of the phosphorylation of MAPKs and IκBα in LPS-induced macrophages (Figure 6).

Notably, phosphorylation of JNK caused by LPS was most significantly inhibited by these compounds. These results suggest that the anti-inflammatory effects of compounds **1**, **9**, and **14** are through the inhibition of activation of MAPKs and I κ B α in LPS-activated macrophages.

Table 4. Inhibitory effects of compounds **1–26** from the stem bark of *F. chinensis* on nitric oxide (NO) generation by RAW264.7 murine macrophages in response to lipopolysaccharide (LPS).

Compounds	IC ₅₀ [μ M] ^a
(8E)-4''-O-Methylglistroside (1)	12.38 \pm 0.86 *
(8E)-4''-O-Methyl demethylglistroside (2)	24.72 \pm 1.25 **
3'',4''-Di-O-methyl demethyloleuropein (3)	37.14 \pm 2.51 *
Olenoside A (4)	>100
(8E)-Ligstroside (5)	42.78 \pm 3.23 *
Oleuropein (6)	40.02 \pm 2.69 *
(8E)-3'',4''-Di-O-methyl oleuropein (7)	53.44 \pm 4.19
Jaspolside methyl ester (8)	65.82 \pm 5.64
Esculetin (9)	9.36 \pm 0.25 **
Copoletin (10)	53.05 \pm 3.63 *
Soscopoletin (11)	15.36 \pm 0.81 *
Esculetin dimethyl ester (12)	31.80 \pm 2.17 *
Raxidin (13)	50.62 \pm 3.08 *
Raxetin (14)	10.11 \pm 0.47 *
Umbelliferone (15)	48.24 \pm 3.22
Methyl isoferulate (16)	>100
Methyl ferulate (17)	>100
Methyl 3,4-dimethoxycinnamate (18)	75.84 \pm 6.28
Methyl (E)- <i>p</i> -coumarate (19)	>100
(E)-Ferulaldehyde (20)	67.38 \pm 4.09
Tyrosol (21)	27.11 \pm 1.87 *
4-Hydroxyphenethyl acetate (22)	35.36 \pm 2.54 *
<i>p</i> -Hydroxybenzaldehyde (23)	55.13 \pm 4.25
(+)-Pinoresinol (24)	41.69 \pm 3.02 *
(+)-Salicifoliol (25)	>100
α -Tocopheryl quinone (26)	>100
Quercetin ^b	33.95 \pm 2.34 *

^a The IC₅₀ values were calculated from the slope of the dose–response curves (SigmaPlot). Values are expressed as mean \pm SEM ($n = 4$) of three independent experiments. * $p < 0.05$, ** $p < 0.01$ compared with the control. ^b Quercetin was used as a positive control.

M2-polarized macrophages are important for tissue repair [34]. Arginase 1 is an important M2 marker that connects Krüppel-like factor 4 (KLF4) to the biologic processes involved in M2 polarization [35]. High levels of arginase-1 can compete with iNOS for arginine and reduce NO production [36]. In addition, KLF4, which is one of the major members of the KLF family, was shown to induce M2 macrophage phenotype, whereas it reduced M1 macrophage expression [37]. We further examined whether compounds **1**, **9**, and **14** enhanced the expression level of M2 macrophages. The result showed that expression levels of arginase-1 and KLF4 were both induced by treatment with compounds **1**, **9**, and **14** (Figure 7). These results suggested that compounds **1**, **9**, and **14** promoted the expression of macrophage M2 markers, arginase-1 and KLF4, and exhibited the anti-inflammatory activity. We can also draw a schematic diagram that shows how compounds **1**, **9**, and **14** influence the polarization of M1 and M2 macrophages (Figure 8).

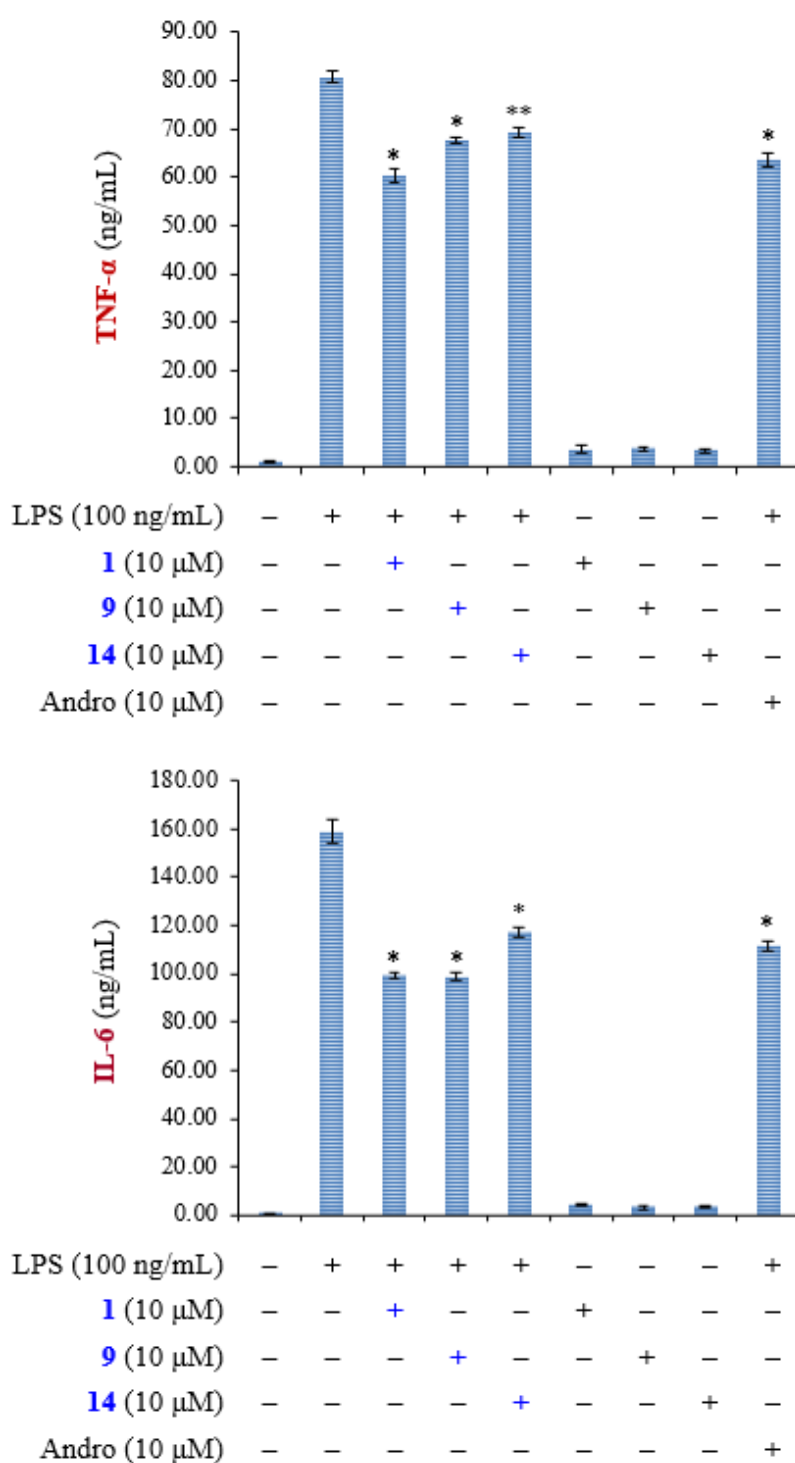


Figure 5. Compounds 1, 9, and 14 suppress the production of proinflammatory cytokines TNF- α and IL-6 in LPS-stimulated RAW 264.7 macrophages. Andrographolide (Andro) was used as positive control. Results are displayed as mean \pm SEM ($n = 3$) of three independent experiments. “+” means treatment with LPS or compound. “-” means no treatment with LPS or compound. Asterisks indicate significant differences (* $p < 0.05$, ** $p < 0.01$) compared with the control.

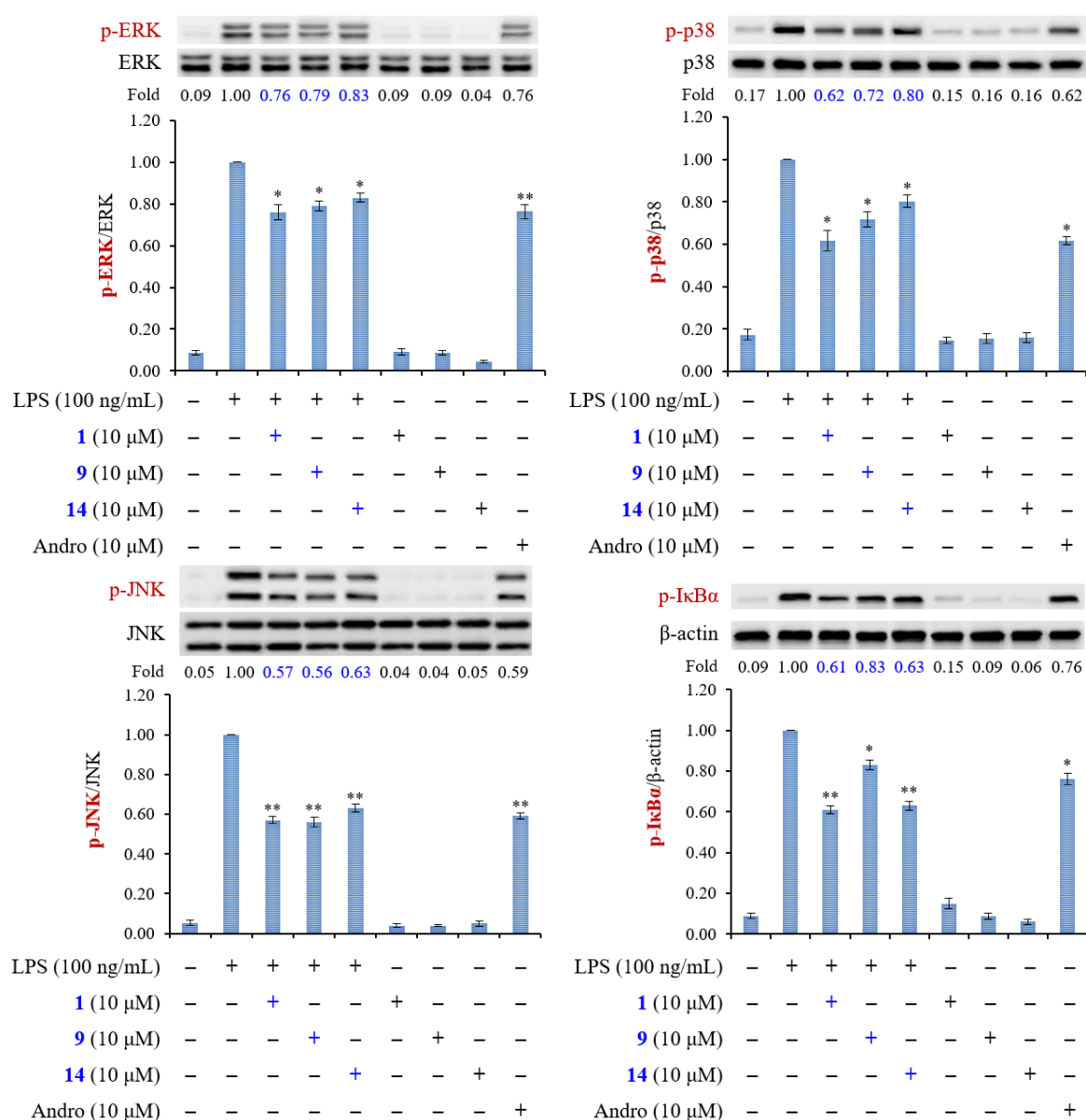


Figure 6. Compounds **1**, **9**, and **14** inhibit the phosphorylation of MAPKs and IκBα in LPS-activated macrophages. RAW264.7 cells were pretreated with **1**, **9**, and **14** (10 μM) for 6 h, and then stimulated with LPS for 15 min. Phosphorylation of MAPKs and IκBα was analyzed by immunoblotting. Densitometric analysis of all samples was normalized to the corresponding total protein or β-actin. Andrographolide (Andro) was used as positive control. Results are displayed as mean ± SEM of three independent experiments. “+” means treatment with LPS or compound. “-” means no treatment with LPS or compound. Asterisks indicate significant differences (* $p < 0.05$ and ** $p < 0.01$) compared with the control.

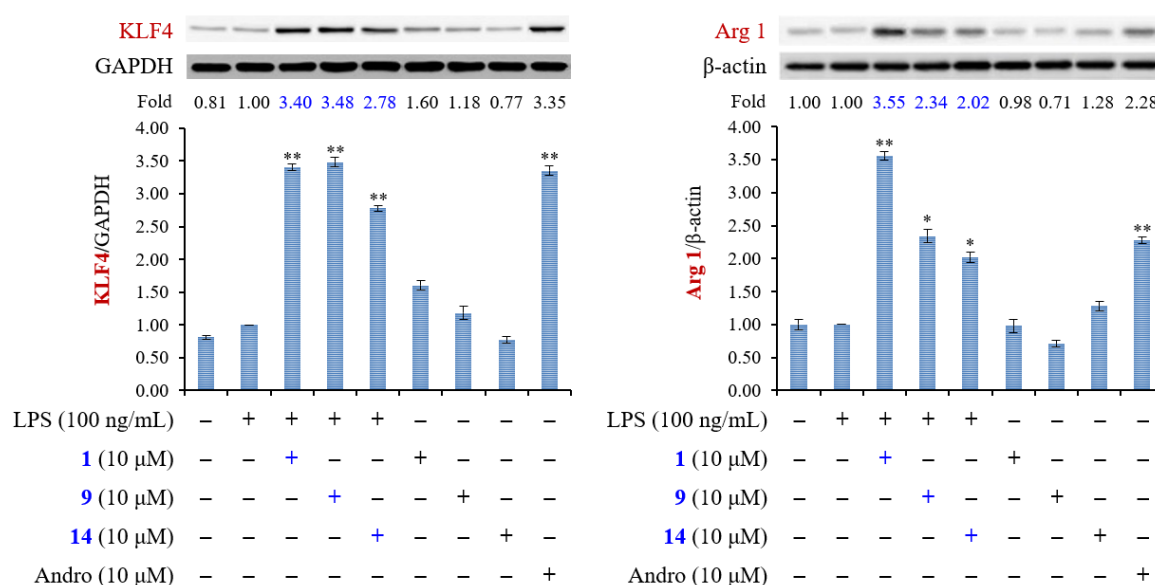


Figure 7. The effect of compounds **1**, **9**, and **14** on M2 polarized macrophages in LPS-stimulated RAW264.7 macrophages. RAW264.7 cells were pretreated with **1**, **9**, and **14** (10 μM) for 6 h, and then stimulated with LPS for 20 h. Expression of KLF4 and arginase 1 (Arg 1) were determined by Western blot analysis. Andrographolide (Andro) was used as positive control. The data were expressed as mean ± SEM of three independent experiments. “+” means treatment with LPS or compound. “-” means no treatment with LPS or compound. Asterisks indicate significant differences (* *p* < 0.05 and ** *p* < 0.01) compared with the control.

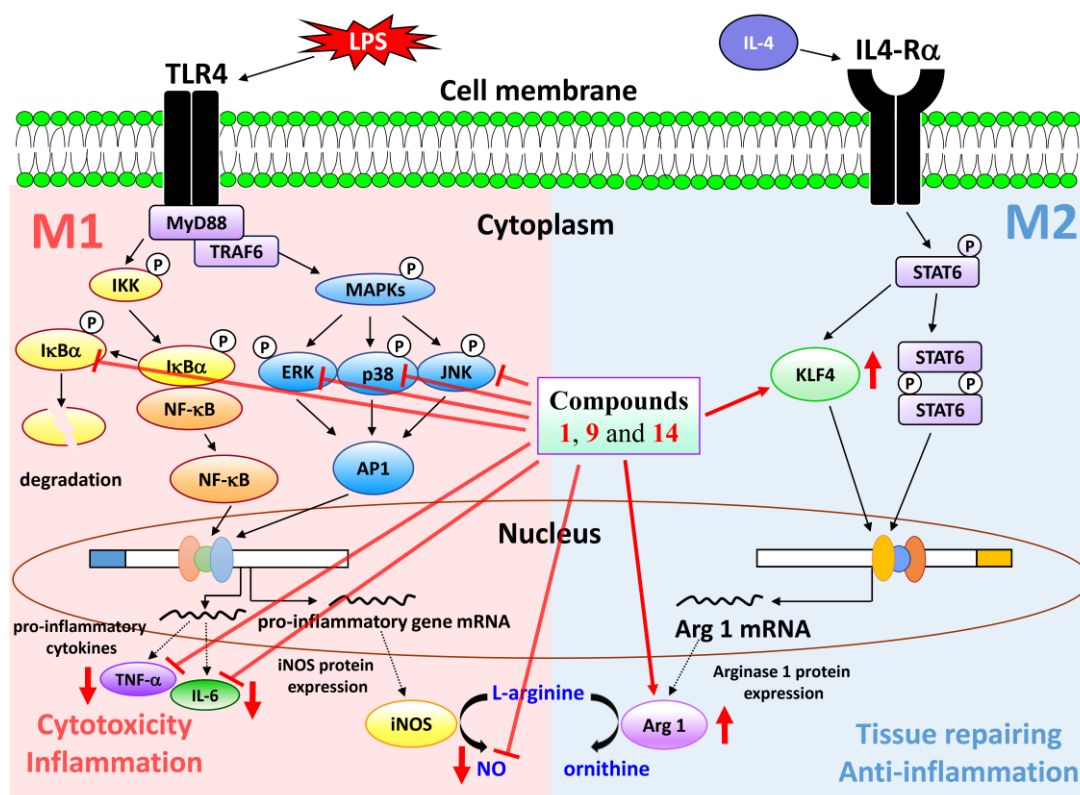


Figure 8. Schematic diagram for anti-inflammatory action of compounds **1**, **9**, and **14** in LPS-induced RAW264.7 macrophages.

3. Materials and Methods

3.1. General Procedures

Melting points were determined on a Yanaco micro-melting point apparatus (Yanaco, Tokyo, Japan) and are uncorrected. Optical rotations were measured using a Jasco DIP-370 polarimeter (Jasco, Easton, MD, USA) in CHCl_3 . Ultraviolet (UV) spectra were obtained on a Jasco UV-240 spectrophotometer (Jasco, Easton, MD, USA). Infrared (IR) spectra (neat or KBr) were recorded on a Perkin Elmer 2000 FT-IR spectrometer (PerkinElmer, Waltham, MA, USA). Nuclear magnetic resonance (NMR) spectra, including correlation spectroscopy (COSY), nuclear Overhauser effect spectrometry (NOESY), rotating frame nuclear Overhauser effect spectrometry (ROESY), heteronuclear multiple-bond correlation (HMBC), and heteronuclear single-quantum coherence (HSQC) experiments, were acquired using a Varian Inova 500 spectrometer operating at 500 MHz (^1H) and 125 MHz (^{13}C), respectively, with chemical shifts given in ppm (δ) using tetramethylsilane (TMS) as an internal standard. Electrospray ionization (ESI) and high-resolution electrospray ionization (HRESI) mass spectra were recorded on a Bruker APEX II mass spectrometer (Bruker, Bremen, Germany). Silica gel (70–230, 230–400 mesh) (Merck, Darmstadt, Germany) was used for column chromatography (CC). Silica gel 60 F-254 (Merck, Darmstadt, Germany) was used for thin-layer chromatography (TLC) and preparative thin-layer chromatography (PTLC).

3.2. Plant Material

The stem bark of *F. chinensis* was collected from Pingtung County, Taiwan, in April 2011 and identified by Prof. J. J. Chen. A voucher specimen (FC 201104) was deposited in the Faculty of Pharmacy, National Yang-Ming University, Taipei, Taiwan.

3.3. Extraction and Isolation

The dried stem bark (4.0 kg) of *F. chinensis* was pulverized and extracted three times with MeOH ($\geq 99\%$, 20 L each) for three days at room temperature. The MeOH extract was concentrated under reduced pressure at 35 °C, and the residue (384 g) was partitioned between EtOAc ($\geq 99.5\%$) and H_2O ($\geq 99.5\%$) (1:1) to provide the EtOAc-soluble fraction (fraction A; 180 g). Fraction A (180 g) was purified by column chromatography (CC) (10 × 72 cm, 7.2 kg of silica gel, 70–230 mesh; CH_2Cl_2 ($\geq 99\%$)/MeOH gradient) to afford 10 fractions: A1 (5 L, CH_2Cl_2), A2 (6 L, $\text{CH}_2\text{Cl}_2/\text{MeOH}$, 90:1), A3 (9 L, $\text{CH}_2\text{Cl}_2/\text{MeOH}$, 80:1), A4 (6 L, $\text{CH}_2\text{Cl}_2/\text{MeOH}$, 60:1), A5 (5 L, $\text{CH}_2\text{Cl}_2/\text{MeOH}$, 50:1), A6 (10 L, $\text{CH}_2\text{Cl}_2/\text{MeOH}$, 40:1), A7 (5 L, $\text{CH}_2\text{Cl}_2/\text{MeOH}$, 20:1), A8 (3 L, $\text{CH}_2\text{Cl}_2/\text{MeOH}$, 10:1), A9 (4 L, $\text{CH}_2\text{Cl}_2/\text{MeOH}$, 1:1), and A10 (2 L, MeOH). Fraction A1 (12.5 g) was subjected to CC (5 × 45 cm, 500 g of silica gel, 230–400 mesh; *n*-hexane/acetone ($\geq 99\%$) 20:1–0:1, 500 mL fractions) to give eight subfractions: A1-1–A1-8. Part (56 mg) of fraction A1-1 was further purified by preparative TLC (silica gel; *n*-hexane (99%)/EtOAc 2:1) to afford 4-hydroxyphenethyl acetate (**22**) (6.6 mg) ($R_f = 0.78$). Part (38 mg) of fraction A1-2 was further purified by preparative TLC (silica gel; *n*-hexane/EtOAc, 1:1) to obtain *p*-hydroxybenzaldehyde (**23**) (4.2 mg) ($R_f = 0.90$). Part (76 mg) of fraction A1-3 was further purified by preparative TLC (silica gel; *n*-hexane/EtOAc, 3:1) to afford (*E*)-ferulaldehyde (**20**) (6.6 mg) ($R_f = 0.25$). Part (105 mg) of fraction A1-5 was further purified by preparative TLC (silica gel; $\text{CH}_2\text{Cl}_2/\text{EtOAc}$, 8:1) to yield (+)-pinoresinol (**24**) (5.5 mg) ($R_f = 0.32$) and (+)-salicifoliol (**25**) (5.6 mg) ($R_f = 0.26$). Part (55 mg) of fraction A1-8 was purified by preparative TLC (silica gel; $\text{CH}_2\text{Cl}_2/\text{acetone}$, 30:1) to obtain α -tocopheryl quinone (**26**) (2.4 mg) ($R_f = 0.73$). Fraction A3 (19.8 g) was subjected to CC (5 × 70 cm, 895 g of silica gel, 230–400 mesh; *n*-hexane/EtOAc 10:1–0:1, 300 mL fractions) to give 10 subfractions: A3-1–A3-10. Part (69 mg) of fraction A3-1 was further purified by preparative TLC (silica gel; *n*-hexane/acetone, 1:1) to afford isoscopoletin (**11**) (2.8 mg) ($R_f = 0.81$). Part (125 mg) of fraction A3-3 was further purified by preparative TLC (silica gel; $\text{CH}_2\text{Cl}_2/\text{MeOH}$, 25:1) to obtain olenoside A (**4**) (7.9 mg) ($R_f = 0.70$) and umbelliferone (**15**) (3.7 mg) ($R_f = 0.70$). Part (71 mg) of fraction A3-4 was further purified by preparative TLC (silica gel; $\text{CH}_2\text{Cl}_2/\text{MeOH}$, 25:1) to afford fraxidin (**13**) (5.2 mg) ($R_f = 0.41$). Part (33 mg)

of fraction A3-8 was further purified by preparative TLC (silica gel; CH₂Cl₂/acetone, 6:1) to yield tyrosol (**21**) (4.9 mg) ($R_f = 0.52$). Part (92 mg) of fraction A3-10 was purified by preparative TLC (silica gel; *n*-hexane/acetone, 1:2) to obtain fraxetin (**14**) (15.9 mg) ($R_f = 0.30$). Fraction A4 (16.7 g) was subjected to CC (5 × 60 cm, 755 g of silica gel, 230–400 mesh; CH₂Cl₂/acetone 10:1–0:1, 1.2 L-fractions) to give eight subfractions: A4-1–A4-8. Part (290 mg) of fraction A4-2 was purified by CC (silica gel, *n*-hexane/acetone 3:2) to afford four subfractions (each 1.2 L, A4-2-1–A4-2-4). Part (43 mg) of fraction A4-2-3 was further purified by preparative TLC (silica gel; CH₂Cl₂/acetone 15:1) to obtain scopoletin (**10**) (3.1 mg) ($R_f = 0.39$). Part (61 mg) of fraction A4-3 was further purified by preparative TLC (silica gel; CH₂Cl₂/acetone, 5:1) to afford aesculetin (**9**) (7.6 mg) ($R_f = 0.46$). Fraction A6 (27.4 g) was subjected to CC (7 × 60 cm, 1.3 kg of silica gel, 230–400 mesh; CH₂Cl₂/EtOAc 10:1–0:1, 1 L-fractions) to give 11 subfractions: A6-1–A6-11. Part (61 mg) of fraction A6-1 was further purified by preparative TLC (silica gel; *n*-hexane/acetone, 5:1) to afford methyl 3,4-dimethoxycinnamate (**18**) (4.3 mg) ($R_f = 0.68$). Part (210 mg) of fraction A6-2 was purified by CC (silica gel, *n*-hexane/acetone 5:1) to afford five subfractions (each 250 mL, A6-2-1–A6-2-5). Part (28 mg) of fraction A6-2-2 was further purified by preparative TLC (silica gel; *n*-hexane/EtOAc, 2:1) to afford methyl ferulate (**17**) (5.7 mg) ($R_f = 0.70$). Part (54 mg) of fraction A6-3 was further purified by preparative TLC (silica gel; CH₂Cl₂/EtOAc, 6:1) to yield methyl isoferulate (**16**) (4.2 mg) ($R_f = 0.38$). Part (56 mg) of fraction A6-4 was purified by preparative TLC (silica gel; *n*-hexane/EtOAc, 2:1) to obtain aesculetin dimethyl ester (**12**) (4.7 mg) ($R_f = 0.71$) and methyl (*E*)-*p*-coumarate (**19**) (3.9 mg) ($R_f = 0.73$). Part (38 mg) of fraction A6-7 was further purified by preparative TLC (silica gel; CHCl₃ (≥99%)/MeOH, 8:1) to afford oleoside methyl ester (**8**) (5.7 mg) ($R_f = 0.19$). Fraction A9 (17.3 g) was subjected to CC (5 × 60 cm, 780 g of silica gel, 230–400 mesh; CH₂Cl₂/MeOH 7:1–0:1, 500 mL fractions) to give 13 subfractions: A9-1–A9-13. Part (75 mg) of fraction A9-4 was further purified by preparative TLC (silica gel; CHCl₃/MeOH, 7:1) to afford (8*E*)-4''-*O*-methylglistroside (**1**) (15.7 mg) ($R_f = 0.66$). Part (63 mg) of fraction A9-5 was further purified by preparative TLC (silica gel; CHCl₃/MeOH, 5:1) to yield (8*E*)-3'',4''-di-*O*-methyloleuropein (**7**) (7.4 mg) ($R_f = 0.53$). Part (108 mg) of fraction A9-7 was purified by CC (silica gel, CHCl₃/MeOH, 3:1) to afford three subfractions (each 150 mL, A9-7-1–A9-7-3). Fraction A9-7-1 (63 mg) was further purified by preparative TLC (silica gel; CHCl₃/MeOH, 4:1) to obtain 3'',4''-di-*O*-methyl demethyloleuropein (**3**) (6.1 mg) ($R_f = 0.61$). Fraction A9-7-2 (28 mg) was further purified by preparative TLC (silica gel; CHCl₃/MeOH, 4:1) to afford (8*E*)-4''-*O*-methyl demethylglistroside (**2**) (7.2 mg) ($R_f = 0.55$). Fraction A10 (36.8 g) was subjected to silica gel column chromatography (10 × 55 cm, 230–400 mesh) with CH₂Cl₂/MeOH, 7:1 to give 14 fractions (each 1.5 L). Part (115 mg) of fraction 10-4 was purified further by preparative TLC (silica gel, CHCl₃/MeOH, 7:1) to afford (8*E*)-ligstroside (**5**) (12.3 mg) ($R_f = 0.65$). Part (132 mg) of fraction 10-5 was purified further by preparative TLC (silica gel, CH₂Cl₂/acetone, 1:2) to yield oleuropein (**6**) (14.6 mg) ($R_f = 0.35$).

(8*E*)-4''-*O*-Methylglistroside (**1**): yellowish oil; $[\alpha]_D^{25}$: −182.2 (*c* 0.2, MOH); UV (MeOH): λ_{\max} (log ϵ) = 238 (4.05), 276 (3.82), 283 (3.81), 318 (3.76) nm; IR (neat): ν_{\max} = 3402 (OH), 1727 (C=O), 1708 (C=O) cm^{−1}; ESI-MS: m/z = 561 [M + Na]⁺; HR-ESI-MS: m/z = 561.1950 [M + Na]⁺ (calcd. for C₂₆H₃₄O₁₂Na: 561.1948). ¹H and ¹³C NMR spectroscopic data, see Table 1.

(8*E*)-4''-*O*-Methyl demethylglistroside (**2**): yellowish oil; $[\alpha]_D^{25}$: −181.5 (*c* 0.25, MOH); UV (MeOH): λ_{\max} (log ϵ) = 225 (4.04), 276 (3.80), 282 (3.79), 317 (3.73) nm; IR (neat): ν_{\max} = 3334 (OH), 1728 (C=O), 1707 (C=O) cm^{−1}; ESI-MS: m/z = 547 [M + Na]⁺; HR-ESI-MS: m/z = 547.1787 [M + Na]⁺ (calcd. for C₂₅H₃₂O₁₂Na: 547.1791). ¹H and ¹³C NMR spectroscopic data, see Table 1.

3'',4''-Di-*O*-methyl demethyloleuropein (**3**): amorphous powder; $[\alpha]_D^{25}$: −155.2 (*c* 0.22, MOH); UV (MeOH): λ_{\max} (log ϵ) = 226 (4.24), 277 (3.40) nm; IR (neat): ν_{\max} = 3350 (OH), 1721 (C=O), 1698 (C=O) cm^{−1}; ESI-MS: m/z = 577 [M + Na]⁺; HR-ESI-MS: m/z = 577.1892 [M + Na]⁺ (calcd. for C₂₆H₃₄O₁₃Na: 577.1897). ¹H and ¹³C NMR spectroscopic data, see Table 1.

3.4. Biological Assay

The activity of the isolated compounds on neutrophil and macrophage proinflammatory response was evaluated by monitoring the inhibition of all isolated compounds against fMLP/CB-induced $O_2^{\bullet-}$ and elastase release and against LPS-induced NO generation in a concentration-dependent manner.

3.4.1. Mensuration of Human Neutrophils

Human neutrophils from venous blood of adult, healthy volunteers (20–27 years old) were isolated by a standard pattern of dextran sedimentation before centrifugation in a Ficoll Hypaque gradient and hypotonic lysis of erythrocytes [38]. Purified neutrophils having >98% viable cells, as detected by the trypan blue exclusion method [39], were resuspended in a calcium (Ca^{2+})-free HBSS buffer at pH 7.4 and were kept at 4 °C prior to use.

3.4.2. Mensuration of Superoxide Anion ($O_2^{\bullet-}$) Generation

The assay for measurement of $O_2^{\bullet-}$ generation was based on the SOD-inhibitable reduction of ferricytochrome *c* [40,41]. In short, after supplementation with 1 mM Ca^{2+} and 0.5 mg/mL ferricytochrome *c*, neutrophils (6×10^5 /mL) were equilibrated at 37 °C for 2 min and incubated with varied concentrations (10–0.01 μ g/mL) of DMSO (as control) or tested compounds 1–26 for 5 min. Cells were incubated with cytochalasin B (1 μ g/mL) for 3 min before the activation with 100 nM formyl-L-methionyl-L-leucyl-L-phenylalanine for 10 min. Changes in absorbance with the reduction of ferricytochrome *c* at 550 nm were constantly detected in a double-beam, six-cell positioner spectrophotometer with continuous stirring (Hitachi U-3010, Tokyo, Japan). Calculations were founded on differences in the reactions with and without SOD (100 U/mL) divided by the extinction coefficient for the reduction of ferricytochrome *c* ($\epsilon = 21.1$ /mM/10 mm).

3.4.3. Measurement of Elastase Release

Degranulation of azurophilic granules was measured by determining elastase release as reported previously [41,42]. Assays were carried out applying MeO-Suc-Ala-Ala-Pro-Val-*p*-nitroanilide as elastase substrate. In brief, after supplementation with MeO-Suc-Ala-Ala-Pro-Val-*p*-nitroanilide (100 μ M), neutrophils (6×10^5 /mL) were equilibrated at 37 °C for 2 min and incubated with tested compounds for 5 min. Cells were treated with fMLP (100 nM)/CB (0.5 μ g/mL), and the changes in absorbance at 405 nm were detected constantly in order to measure elastase release. The results were displayed as the percent of elastase release in the fMLP/CB-activated, drug-free control system.

3.4.4. Determination of NO Production

NO production was indirectly assessed by measuring the nitrite levels in the cultured media and serum determined by a colorimetric method based on the Griess reaction. RAW264.7 cells were pretreated with compounds for 1 h, and then stimulated with LPS (100 ng/mL) for 20 h at 37 °C. Then, cells were dispensed into 96-well plates, and 100 μ L of each supernatant was mixed with the same volume of Griess reagent (1% sulfanilamide, 0.1% naphthylethylenediamine dihydrochloride, and 5% phosphoric acid) and incubated at room temperature for 10 min; the absorbance was measured at 540 nm with a Micro-Reader (Molecular Devices). By using sodium nitrite to generate a standard curve, the concentration of nitrite was measured from absorbance at 540 nm [43].

3.4.5. Cell Viability Assay

Cells (4×10^5) were cultured in 96-well plates containing DMEM supplemented with 10% FBS for one day to become nearly confluent. Then, cells were cultured with compounds 1–26 in the presence of 100 ng/mL LPS (lipopolysaccharide) for 24 h. After that, the cells were washed twice with DPBS and incubated with 100 μ L of 0.5 mg/mL MTT for 2 h at 37 °C testing for cell viability. The medium was then

discarded and 100 μ L dimethyl sulfoxide (DMSO) was added. After 30 min incubation, absorbance at 570 nm was read using a microplate reader (Molecular Devices, Sunnyvale, CA, USA) [44].

3.4.6. Enzyme-Linked Immunosorbent Assay

RAW264.7 cells (4×10^5 cells in 96-well plates) were pretreated with compounds **1**, **9**, **14**, or vehicle (0.05% DMSO) for 1 h and then stimulated with LPS (100 ng/mL) for 20 h. Supernatants were collected and analyzed for production of TNF- α and IL-6 by using appropriate ELISA kits (R&D, MN, USA) in accordance with the manufacturer's instructions.

3.4.7. Western Blot

Western blot analysis followed as previously described with slight changes [45]. Cells (1.0×10^6) were seeded into 6 cm dishes and grown until 80–85% confluent. RAW264.7 cells were pretreated with **1**, **9**, and **14** (10 μ M) for 6 h, and then stimulated with LPS (100 ng/mL) for 15 min (for detecting p-I κ B α , p-ERK, p-JNK, and p-p38) or 20 h (for detecting arginase 1 and KLF4) at 37 $^{\circ}$ C. Cultured medium was removed and cells were washed with ice-cold PBS. After RIPA buffer (Cell Signaling, MA, USA) was added, cells were scraped off the plate and transferred to the Eppendorf on ice immediately. The proteins were quantified using the BCA protein assay. Cells were preserved at -80° C overnight and then centrifuged (15,000 \times rpm, 30 min, 4 $^{\circ}$ C). Equal amounts of protein samples (25 μ g) and prestained protein marker were loaded onto SDS-PAGE. After being stacked at 80 V and separated at 100 V, the proteins were transferred onto the polyvinylidene fluoride (PVDF) membranes at 350 mA. The PVDF membranes were blocked with 5% (*w/v*) of BSA with Tris-buffered saline (TBST) containing 0.1% (*v/v*) Tween 20 at room temperature for 1 h and washed three times with TBST for 15 min each time. Primary antibodies were incubated with the membranes overnight, shaking at 4 $^{\circ}$ C. Then, each membrane was washed with TBST and incubated with horseradish peroxidase (HRP)-conjugated secondary antibodies at room temperature for 1 h while shaking. Finally, each membrane was developed using an ECL detection kit, and the images were visualized by ImageQuant LAS 4000mini (GE Healthcare, MA, USA). Images were quantified using Image J version 1.48 (NIH, Bethesda, MD, USA).

3.4.8. Statistical Analysis

Results are expressed as the mean \pm SEM, and comparisons were made using Tukey's HSD test. A probability of 0.05 or less was considered significant. The software SigmaPlot was used for the statistical analysis.

4. Conclusions

Twenty-six compounds, including three undescribed secoiridoid glucosides, (8*E*)-4''-*O*-methylligstroside (**1**), (8*E*)-4''-*O*-methyldemethylligstroside (**2**), and 3''-4''-*di-O*-methyldemethyl-oleuropein (**3**), were isolated from stem bark of *F. chinensis*. The structures of these isolates were elucidated according to spectroscopic data. The effects on neutrophil proinflammatory responses of isolates were evaluated by suppressing fMLP/CB-induced $O_2^{\bullet-}$ generation and elastase release by human neutrophils. The results of anti-inflammatory assays show that compounds **1**, **9**, **11**, **14**, **21**, and **22** can obviously inhibit fMLP-induced $O_2^{\bullet-}$ generation and/or elastase release. (8*E*)-4''-*O*-Methylligstroside (**1**) and fraxetin (**14**) were the most effective among the isolated compounds, with IC_{50} values of 0.08 ± 0.01 and 0.50 ± 0.10 μ g/mL, respectively, against fMLP-induced $O_2^{\bullet-}$ generation and elastase release. Furthermore, compounds **9** and **14** showed potent inhibition with IC_{50} values of 9.36 ± 0.25 and 10.11 ± 0.47 μ M, respectively, against LPS-induced NO generation. Compounds **1**, **9**, and **14** suppressed LPS-induced NO, TNF- α , and IL-6 generation via blocking the phosphorylation of MAPKs and degradation of I κ B α . In addition, compounds **1**, **9**, and **14** stimulated anti-inflammatory M2 phenotype by elevating the expression of arginase 1 and KLF4. In conclusion, compounds **1**, **9**, and **14** interfered with multiple intracellular targets. Our research indicates *F. chinensis* and its constituents (especially **1**,

9, and 14) may deserve further investigation as potential candidates for the treatment or prevention of various inflammatory diseases.

Supplementary Materials: Supplementary materials are available online, Figures S1–S9: ESIMS, HRESIMS, 1D, and 2D NMR spectra for (8E)-4''-O-methylgigstroside (1), Figures S10–S18: ESIMS, HRESIMS, 1D, and 2D NMR spectra for (8E)-4''-O-methyl-demethylgigstroside (2), Figures S19–S27: ESIMS, HRESIMS, 1D, and 2D NMR spectra for 3'',4''-di-O-methyl-demethyloleuropein (3).

Author Contributions: H.-C.C., S.-W.W., T.-L.H., M.-J.C., P.-J.S., and K.-W.L. performed the bioassay and analyzed the data. C.-Y.C. conducted the isolation and structure elucidation of the constituents. J.-J.C. planned, designed, and organized all of the research of this study and the preparation of the manuscript. All authors have read and agreed to the published version of the manuscript.

Funding: This research was supported by grants from the Ministry of Science and Technology, Taiwan (No. MOST 106-2320-B-010-033-MY3 and MOST 109-2320-B-010-029-MY3), awarded to Prof. J.-J. Chen.

Conflicts of Interest: The authors declare no conflict of interest.

References

1. Wei, Z.; Green, S.P. *Fraxinus chinensis* in *Flora of China*; Science Press: Beijing, China, 1996; Volume 15, p. 277.
2. Huang, Y.L.; Opong, M.B.; Guo, Y.; Wang, L.Z.; Fang, S.M.; Deng, Y.R.; Gao, X.M. The Oleaceae family: A source of secoiridoids with multiple biological activities. *Fitoterapia* **2019**, *136*, 104155. [[CrossRef](#)] [[PubMed](#)]
3. Takenaka, Y.; Tanahashi, T.; Shintaku, M.; Sakai, T.; Nagakura, N.; Parida. Secoiridoid glucosides from *Fraxinus americana*. *Phytochemistry* **2000**, *55*, 275–284. [[CrossRef](#)]
4. Xiao, K.; Song, Q.H.; Zhang, S.W.; Xuan, L.J. Water-soluble constituents of the root barks of *Fraxinus rhynchophylla* (Chinese drug Qinpi). *J. Asian Nat. Prod. Res.* **2008**, *10*, 205–210. [[CrossRef](#)] [[PubMed](#)]
5. Zhang, D.M.; Wnag, L.L.; Li, J.; Hu, L.H. Two new coumarins from *Fraxinus chinensis* Roxb. *J. Integr. Plant Biol.* **2007**, *31*, 1277–1280.
6. Wang, L.J.; Sun, F.; Zhang, X.Y.; Ma, Z.J.; Cheng, L. A secoiridoid with quinone reductase inducing activity from *Cortex fraxini*. *Fitoterapia* **2010**, *81*, 834–837. [[CrossRef](#)] [[PubMed](#)]
7. Lee, D.G.; Choi, J.S.; Yeon, S.W.; Cui, E.J.; Park, H.J.; Yoo, J.S.; Chung, I.S.; Baek, N.L. Secoiridoid glycoside from the flowers of *Osmanthus fragrans* var. *aurantiacus* Makino inhibited the activity of β -secretase. *J. Korean Soc. Appl. Biol. Chem.* **2010**, *53*, 371–374. [[CrossRef](#)]
8. Darmak, N.; Allouche, N.; Hamdi, B.; Litaudon, M.; Darmak, M. New secoiridoid from olive mill wastewater. *Nat. Prod. Res.* **2012**, *26*, 125–131. [[CrossRef](#)]
9. Tanahashi, T.; Takenaka, Y.; Nagakura, N. Two dimeric secoiridoid glycosides from *Jasminum polyanthum*. *Phytochemistry* **1996**, *41*, 1341–1345. [[CrossRef](#)]
10. He, Z.D.; But, P.H.; Chan, T.W.; Dong, H.; Xu, H.X.; Lau, C.P.; Sun, H.D. Antioxidative glucosides from the fruits of *Ligustrum lucidum*. *Chem. Pharm. Bull.* **2001**, *49*, 780–784. [[CrossRef](#)]
11. Shen, Y.C.; Lin, S.L.; Hsieh, P.W.; Chein, C.C. Secoiridoid glycosides from *Jasminum polyanthum*. *J. Chin. Chem. Soc.* **1996**, *43*, 171–176. [[CrossRef](#)]
12. Tsukamoto, H.; Hisada, S.; Nishibe, S.; Rouxt, D.G.; Rourke, J.P. Coumarin from *Olea Africana* and *Olea capensis*. *Phytochemistry* **1984**, *23*, 699–700. [[CrossRef](#)]
13. Wu, T.S.; Shi, L.S.; Wang, J.J.; Iou, S.C.; Chang, H.C.; Chen, Y.P.; Kuo, Y.H.; Chang, Y.L.; Teng, C.M. Cytotoxic and antiplatelet aggregation principles of *Ruta graveolens*. *J. Chin. Chem. Soc.* **2003**, *50*, 171–178. [[CrossRef](#)]
14. Lee, C.K.; Lee, P.H.; Kuo, Y.H. The chemical constituents from the aril of *Cassia fistula* L. *J. Chin. Chem. Soc.* **2001**, *48*, 1053–1058. [[CrossRef](#)]
15. Yu, H.J.; Chen, C.C.; Shieh, B.J. The constituents from the leaves of *Magnolia coco*. *J. Nat. Prod.* **1998**, *61*, 1017–1019. [[CrossRef](#)]
16. Kaufmann, F.; Lam, J. Chemical constituents of the genus of *Dahlia* II. The isolation of two new aromatic compounds: Naringenin trimethylether and fraxedin. *Acta Chem. Scand.* **1967**, *21*, 311–313. [[CrossRef](#)]
17. Aiyelaagbe, J.B.; Gloer, J.B. Japodic acid, a novel aliphatic acid from *Jatropha podagrica* Hook. *Rec. Nat. Prod.* **2008**, *2*, 100–106.

18. Kumar, S.; Ray, A.B.; Konno, C.; Oshima, Y.; Hikino, H. Cleomiscosin D, a coumarinolignan from seeds of *Cleome viscosa*. *Phytochemistry* **1988**, *27*, 636–638. [[CrossRef](#)]
19. Weight, E.S.; Razdan, T.K.; Qadni, B.; Harkar, S. Chromones and coumarin from *Skimmia larueola*. *Phytochemistry* **1982**, *26*, 2063–2069. [[CrossRef](#)]
20. Rose, B.R.; Kaustuv, B. Anullmann ether reaction involving an alkynyl substrate: A convergent route to a combretastatin intermediate. *Synth. Commun.* **1995**, *25*, 3187–3197.
21. Lee, T.H.; Chiou, J.L.; Lee, C.K.; Kuo, Y.H. Separation and determination of chemical constituents in the root of *Rhus javanica* L. var. *roxburghiana*. *J. Chin. Chem. Soc.* **2005**, *52*, 833–841. [[CrossRef](#)]
22. Bowden, B.F.; Camie, R.C.; Parnell, J.C. Constituents of the fruit of *Pseudopanax arboreum* (Araliaceae). *Aust. J. Chem.* **1975**, *28*, 91–107. [[CrossRef](#)]
23. Gopalakrishnan, S.; Subbarao, G.V.; Nakahara, K.; Yoshihashi, T.; Ito, O.; Maeda, I.; Ono, H.; Yoshida, M. Nitric oxide inhibitors from root tissues of *Brachiaria humidicola*, a tropical grass. *J. Agric. Food. Chem.* **2007**, *55*, 1385–1388. [[CrossRef](#)] [[PubMed](#)]
24. Barakat, H.H.; Nawwar, M.A.M.; Buddrust, J.; Linscheid, M. Niloticol, a phenolic glyceride and two phenolic aldehydes from the roots of *Tamarix nilotica*. *Phytochemistry* **1987**, *26*, 1837–1838. [[CrossRef](#)]
25. Xu, Q.M.; Liu, Y.L.; Li, X.R.; Feng, Y.L.; Yang, S.L. Two new phenylglycol derivatives isolated from *Syringa reticulata* var. *mandshurica* and their antifungal activities. *Chem. Pharm. Bull.* **2009**, *57*, 863–866. [[CrossRef](#)]
26. Assia, I.; Bouaziz, M.; Ghamgui, H.; Kamoun, A.; Miled, N.; Sayadi, S.; Gargouri, Y. Optimization of lipase-catalyzed synthesis of acetylated tyrosol by response surface methodology. *J. Agric. Food Chem.* **2007**, *55*, 10298–10305. [[CrossRef](#)]
27. Chiang, C.Y.; Leu, Y.L.; Chan, Y.Y.; Wu, T.S. Sodium aristolochates from the flowers and fruits of *Aristolochia zollingeriana*. *J. Chin. Chem. Soc.* **1998**, *45*, 93–97. [[CrossRef](#)]
28. El-Hassan, A.; El-Sayed, M.; Hamed, A.I.; Rhee, I.K.; Ahmed, A.A.; Zeller, K.P.; Verpoorte, R. Bioactive constituents of *Leptadenia arborea*. *Fitoterapia* **2003**, *74*, 184–187. [[CrossRef](#)]
29. Marchand, P.A.; Zajick, J.; Lewis, N.G. Oxygen insertion in *Sesamum indicum* furanofuran lignans. Diastereoselective syntheses of enzyme substrate analogues. *Can. J. Chem.* **1997**, *75*, 840–849. [[CrossRef](#)]
30. Chang, M.H.; Wang, G.J.; Kuo, Y.H.; Lee, C.K. The low polar constituents from *Bidens pilosa* L. var. *minor* (Blume) Sherff. *J. Chin. Chem. Soc.* **2000**, *47*, 1131–1136. [[CrossRef](#)]
31. Borregaard, N. The human neutrophil. Function and dysfunction. *Eur. J. Haematol.* **1998**, *41*, 401–413. [[CrossRef](#)]
32. Roos, D.; van Bruggen, R.; Meischl, C. Oxidative killing of microbes by neutrophils. *Microbes Infect.* **2003**, *5*, 1307–1315. [[CrossRef](#)] [[PubMed](#)]
33. Witko-Sarsat, V.; Rieu, P.; Descamps-Latscha, B.; Lesavre, P.; Halbwachs-Mecarelli, L. Neutrophils: Molecules, functions and pathophysiological aspects. *Lab. Investig.* **2000**, *80*, 617–653. [[CrossRef](#)] [[PubMed](#)]
34. Benoit, M.; Desnues, B.; Mege, J.L. Macrophage polarization in bacterial infections. *J. Immunol. Res.* **2008**, *181*, 3733–3739. [[CrossRef](#)] [[PubMed](#)]
35. Pauleau, A.L.; Rutschman, R.; Lang, R.; Pernis, A.; Watowich, S.S.; Murray, P.J. Enhancer-mediated control of macrophage-specific arginase I expression. *J. Immunol.* **2004**, *172*, 7565–7573. [[CrossRef](#)] [[PubMed](#)]
36. Yang, Z.; Ming, X.F. Functions of arginase isoforms in macrophage inflammatory responses: Impact on cardiovascular diseases and metabolic disorders. *Front. Immunol.* **2014**, *5*, 533. [[CrossRef](#)]
37. Liao, X.; Sharma, N.; Kapadia, F.; Zhou, G.; Lu, Y.; Hong, H.; Paruchuri, K.; Mahabeleshwar, G.H.; Dalmas, E.; Venteclef, N.; et al. Krüppel-like factor 4 regulates macrophage polarization. *J. Clin. Investig.* **2011**, *121*, 2736–2749. [[CrossRef](#)]
38. Boyum, A. Isolation of mononuclear cells and granulocytes from human blood. Isolation of mononuclear cells by one centrifugation, and of granulocytes by combining centrifugation and sedimentation at 1 g. *Scand. J. Clin. Lab. Investig.* **1968**, *97*, 77–89.
39. Jauregui, H.O.; Hayner, N.T.; Driscoll, J.L.; Williams-Holland, R.; Lipsky, M.H.; Galletti, P.M. Trypan blue dye uptake and lactate dehydrogenase in adult rat hepatocytes—freshly isolated cells, cell suspensions, and primary monolayer cultures. *In Vitro* **1981**, *17*, 1100–1110. [[CrossRef](#)]
40. Babior, B.M.; Kipnes, R.S.; Curnutte, J.T. Biological defense mechanisms. The production by leukocytes of superoxide, a potential bactericidal agent. *J. Clin. Investig.* **1973**, *52*, 741–744. [[CrossRef](#)]

41. Hwang, T.L.; Leu, Y.L.; Kao, S.H.; Tang, M.C.; Chang, H.L. Viscolin, a new chalcone from *Viscum coloratum*, inhibits human neutrophil superoxide anion and elastase release via a cAMP-dependent pathway. *Free Radic. Biol. Med.* **2006**, *41*, 1433–1441. [[CrossRef](#)]
42. Chen, J.J.; Ting, C.W.; Wu, Y.C.; Hwang, T.L.; Cheng, M.J.; Sung, P.J.; Wang, T.C.; Chen, J.F. New labdane-type diterpenoids and anti-inflammatory constituents from *Hedychium Coronarium*. *Int. J. Mol. Sci.* **2013**, *14*, 13063–13077. [[CrossRef](#)] [[PubMed](#)]
43. Johansson, M.; Köpcke, B.; Anke, H.; Sterner, O. Biologically active secondary metabolites from the ascomycete A111-95. 2. Structure elucidation. *J. Antibiot.* **2002**, *55*, 104–106. [[CrossRef](#)] [[PubMed](#)]
44. Mosmann, T. Rapid colorimetric assay for cellular growth and survival: Application to proliferation and cytotoxicity assays. *J. Immunol. Methods* **1983**, *65*, 55–63. [[CrossRef](#)]
45. Lai, J.L.; Liu, Y.H.; Liu, C.; Qi, M.P.; Liu, R.N.; Zhu, X.F.; Zhou, Q.G.; Chen, Y.Y.; Guo, A.Z.; Hu, C.M. Indirubin inhibits LPS-induced inflammation via TLR4 abrogation mediated by the NF- κ B and MAPK signaling pathways. *Inflammation* **2017**, *40*, 1–12. [[CrossRef](#)] [[PubMed](#)]

Sample Availability: Samples of the compounds are available from the authors.

Publisher's Note: MDPI stays neutral with regard to jurisdictional claims in published maps and institutional affiliations.



© 2020 by the authors. Licensee MDPI, Basel, Switzerland. This article is an open access article distributed under the terms and conditions of the Creative Commons Attribution (CC BY) license (<http://creativecommons.org/licenses/by/4.0/>).